Dissolved organic matter does not promote glyphosate degradation in auto-heterotrophic aquatic microbial communities

Joan Artigas, Isabelle Batisson, Louis Carles

DISSOLVED ORGANIC MATTER DOES NOT PROMOTE GLYPHOSATE DEGRADATION IN AUTO-HETEROTROPHIC AQUATIC MICROBIAL COMMUNITIES

Joan Artigas, Isabelle Batisson, Louis Carles

Université Clermont Auvergne, CNRS, Laboratoire Microorganismes : Génome et Environnement, F-63000 Clermont–Ferrand, France.

Corresponding author address:
J Artigas
UNIVERSITE CLERMONT AUVERGNE
Campus Universitaire des Cézeaux
1 Impasse Amélie Murat
63178 AUBIERE Cedex
Tél. +33 473 40 74 73 Fax. +33 473 40 76 70
E-mail : joan.artigas_alejo@uca.fr

Summary

Environmental dissolved organic matter (DOM) has been proved to increase microbial population sizes and stimulate the degradation of some pesticide molecules. Among these molecules, the present study investigated the biodegradation of the herbicide glyphosate depending on photoautotrophs DOM supply in a microbial consortium isolated from river biofilms. Degradation experiments in the laboratory were performed in dark and light conditions, as well as after antibiotic supply, in order to characterize the eventual interactions between photoautotrophs and heterotrophs activity during glyphosate degradation. Fifty percent of the initial concentration of glyphosate (0.6 mM) was transformed into aminomethyl phosphonic acid (AMPA) after 9 days in presence or absence of light. Accordingly, the photoautotrophic DOM supply was not stimulating glyphosate degradation by microbial heterotrophs. This lack of response was probably explained by the low net primary production values and weak dissolved organic carbon production recorded in light treatments. The supply of the antibiotic drastically stopped glyphosate transformation demonstrating the central role of bacteria in the biodegradation of the herbicide. Glyphosate also modified the structure of prokaryotes assemblages in the consortium by increasing the relative abundances of Alphaproteobacteria and slightly decreasing those of Gammaproteobacteria. The chemoorganotrophic bacteria *Phenylobacterium* sp. (Alphaproteobacteria) was related to the transformation of glyphosate in our microbial consortium. The present study highlights the complexity of microbial interactions between photoautotrophs and heterotrophs in microbial assemblages that can contribute to the degradation of pesticides present in aquatic environments.

Capsule

The interaction with DOM of photoautotrophic origin did not influence bacterial degradation of glyphosate.

Keywords

Alphaproteobacteria, aminomethyl phosphonic acid, biodegradation, biofilm, dissolved organic matter.

Introduction

Microorganisms exploiting specific interactions to increase ecological performance often co-aggregate in nature, while microorganisms that antagonize each other will tend to spatially segregate (Cordero and Datta 2016). Metabolites exchange among neighboring cells has been demonstrated in bacterial cross-feeding experiments in the laboratory (*e. g.* Mee et al. 2014). This phenomenon has been also described for natural aquatic microbial communities where exchanges take place between cells of different microbial groups. In auto-heterotrophic microbial communities, algal production has been demonstrated to influence bacterial productivity through the release of dissolved organic matter (Søndergaard et al. 1985, Espeland et al. 2001) mostly resulting from growth and lysis of the cells and/or the extracellular rejection of unprocessed substrates due to stoichiometric constraints in the former (Carlson and Hansell 2015). Algal contributions to environmental dissolved organic matter (DOM) are non-negligible ranging from 5% (in humic systems) to 40% (in nutrient enriched systems) of the total dissolved organic carbon pool (Bade et al. 2007). Kovárová-kovar and Egli (1998) proposed that mixed carbon sources at low concentrations present in environmental DOM might be used simultaneously by microbes and will lead to growth and increased population sizes hereby reducing lag times and increasing degradation rates of pesticides.

The quantity and quality of environmental DOM, including the extracellular algal release, has been proved to influence pesticide biodegradation. For instance, effects of DOM on linuron degradation were observed at high linuron concentrations (10 mg L^{-1}) with individual *Variovorax sp*. strain cultures (Horemans et al. 2012). Linuron biodegradation was inhibited in the presence of easily degradable carbon substrate (explained by carbon catabolite repression) but stimulated after supplementation of environmental DOM. In fact, the concentrations of carboxylic acids and carbohydrates in environmental DOM were relatively low and did not repress but stimulate linuron degradation. Polycyclic aromatic hydrocarbon (phenanthrene) biodegradation by *Sphingomonas sp*. LH162 was also enhanced in the presence of environmental DOM (*ex*. humic acids, Smith et al. 2009). In this case, environmental DOM acted as a carrier of phenantrene (generating DOM-phenantrene complexes) increasing the total phenantrene flux to *Sphingomonas*'s cells. According to these observations, our study sought to elucidate the influence of environmental DOM of photoautotrophic origin on the biodegradation of the ubiquitous herbicide glyphosate.

Glyphosate (*N*-(phosphonomethyl) glycine) is a systemic herbicide exhibiting a broad activity spectrum, and is one of the most-used active substances worldwide. This molecule

and its main metabolite, the aminomethyl phosphonic acid (AMPA), are among the most often quantified compounds in surface waters from Europe (ex. Carles et al. 2019). In this generalized contamination context, studies revealing the presence of substantial glyphosate residues concentrations in urine samples of both humans and animals in Germany and Denmark (Krüger et al. 2014) have arisen concern of European citizens and authorities regarding the regulation in the use of this molecule and its mitigation from the environment. Microbial degradation appears as the main process explaining the dissipation of glyphosate from soils and wastewaters (Gimsing et al. 2004 and Obojska et al. 1999, respectively). Degradation of glyphosate by microbes proceeds by two different pathways (Figure S1). In the first metabolic pathway, the C-P bond of glyphosate is initially cleaved by a C-P lyase enzyme resulting in the release of a phosphate group and a molecule of sarcosine (Shinabarger and Braymer, 1986). Only certain microbial species subjected to strong phosphorus starvation, which rarely occurs in natural environments, are capable to cleave the C-P bond in the glyphosate molecule in order to obtain phosphorus (Pipke and Amrhein 1988, Carles et al. 2019). The sarcosine can be further enzyme-oxidized into glycine and formaldehyde. In the second metabolic pathway, glyphosate is degraded by cleavage of the C-N bond releasing equimolar quantities of AMPA and glyoxylate. This pathway is the most observed both in natural environments (soil and water bodies) and in waste treatment facilities (Sviridov et al. 2015). The metabolite AMPA can be later transformed into phosphate and methylamine by the action of a C-P lyase and/or into phosphate and formaldehyde by the joint action of a transaminase and a phosphonatase.

A recent review highlighted that most of glyphosate-degrading strains use glyphosate as P and/or N source while very few as a C source (Zhan et al. 2018). This is the case of *Achromobacter sp*. LW9 and *Agrobacterium radiobacter* SW9 which can use glyphosate as a sole carbon source in presence of phosphate by means of the AMPA degradation pathway (McAuliffe et al. 1990). In the present study, we investigated the influence of photoautotrophic DOM production on the capacity of heterotrophic microbes for degrading glyphosate. The microbial assemblage used in this study was isolated from river biofilms capable to transform glyphosate via the AMPA pathway (Carles et al. 2019) that were further adapted to use glyphosate as main carbon source. We tested two specific hypotheses: i) light availability would promote photoautotrophs DOM production, and therefore, stimulate glyphosate biodegradation, and ii) the supply of an antibiotic will reduce glyphosate biodegradation, unless antibiotic-resistant bacteria in the microbial assemblage continue the degradation process.

Materials and methods

Chemical reagents

Glyphosate (PESTANAL, analytical standard ≥ 98%) was purchased from Sigma-Aldrich (France). Enrichment-culture approach was performed on MOPS synthetic media composed of 3-(N-Morpholino)propanesulfonic acid, 4-Morpholinepropanesulfonic acid (MOPS, 40 mM), tricine (4 mM), $FeSO_4$ (10 µM), K_2SO_4 (276 µM), $CaCl_2$ (0.5 µM), $MgCl_2$ (525 µM), NaCl (50 mM), $(NH4)_6Mo_7O_{24}.4H_2O$ (30 nM), H_3BO_3 (4 µM), $CoCl_2.6H_2O$ (0.3 µM), $CuSO_4.5H_2O$ (0.1 µM), $MnCl_2.4H_2O$ (0.8 µM), $ZnSO_4.7H_2O$ (0.1 µM), Thiamine HCl (0.3 µM), K_2HPO_4 (1.32 mM), NH_4Cl (9.5 mM) supplemented with glyphosate at 0.6, 10, and 20 mM**.** pH was adjusted in all cases to 7.4. Chloramphenicol (170 mg L^{-1} in ethanol) was supplemented to antibiotic treatments at a final concentration of 0.5 mg L^{-1}.

Microbial consortium

Enrichment cultures were performed from downstream river biofilms of the Artière (biofilms exposed to 100 µg glyphosate L^{-1} and 100 µg Phosphorus L^{-1}, Carles et al. 2019) with increasing the concentration of glyphosate (0.6, 10, and 20 mM) used as main carbon source. Each enrichment step was 21 days long except for the last one which lasted for 36 days. The flasks were incubated at 19 ± 0.1 °C in an orbital shaker at 100 rpm, and the photoperiod was set at 13 h light: 11 h dark. Before the starting of degradation experiments, the microbial consortium was acclimated back to relatively low glyphosate concentration (0.6 mM) after two repeated sub-culturing steps at 0.6 mM for 30 days each. This final microbial consortium was the one used for the experimental treatments described below.

Experimental setup

The influence of light availability (Light and Dark) and bacteria (with or without Antibiotic) on microbial degradation of glyphosate was tested in a full factorial experiment. Experimental treatments were i) glyphosate in light and dark conditions (Light_Gly and Dark_Gly), ii) glyphosate + chloramphenicol in light and dark conditions (Light_Gly_Antibiotic and Dark_Gly_Antibiotic), iii) microbial consortium without glyphosate in light and dark conditions (Light_Control and Dark_Control), and iv) abiotic controls with glyphosate and without microbial consortium in light and dark conditions (Light_Abiotic and Dark_Abiotic). Each experimental treatment was prepared in triplicate in 250 mL culture flasks (Falcon

Corning®, ref. 353135). The glyphosate treatment was prepared after mixing 99 mL MOPS-glyphosate (0.6 mM) + 1 mL of microbial consortium. The antibiotic treatment was prepared in the same manner but adding chloramphenicol (98.7 mL MOPS-glyphosate (0.6 mM) + 1 mL consortium + 0.294 mL chloramphenicol (0.5 mg L^{-1})). And finally, the abiotic control consisted of 100 mL MOPS glyphosate (0.6 mM), while the biotic control consisted of 99 mL MOPS without glyphosate + 1 mL microbial consortium. Each treatment was incubated in dark (24 h dark at 0 Lux) or light conditions (13 h light (1450-1500 Lux): 11 h dark (0 Lux)) in a thermo-regulated chamber set at 19 +/- 0.1 °C under orbital agitation (100 rpm). The culture in the different treatments was sampled at days 0, 4, 7, 9, 11, 14, 16, and 18 after inoculation of the microbial consortium.

Glyphosate and metabolites analyses

Glyphosate and AMPA quantification was performed on 1 mL media samples collected directly from culture flasks at all sampling dates. After 5 min centrifugation at 13000 *g*, supernatants were directly transferred to HPLC vials in which a derivatization step with 9-fluorenylmethoxycarbonyl chloride (FMOC, 97%, Sigma-Aldrich) was conducted (Wang et al. 2016). The derivatization consisted in mixing 500 µL of sample (1/10 diluted in ultra-pure water) with 150 µL borate buffer 0.2 M pH 8.85 and 150 µL FMOC-Cl 6 mM in acetonitrile. After 1 h derivatization in the dark, 200 µL of pure methanol (HPLC grade ≥ 99.9% purity, Sigma-Aldrich) were added to samples that were further analyzed by liquid chromatography (Waters system coupled to a 474 Scanning Fluorescence Detector). Separation was achieved by a C18 Phenomenex Kinetex EVO column (5 µm 150 × 4.6 mm). The mobile phases consisted of 5 mM ammonium acetate (pH = 9) solvent A and methanol solvent B. The elution gradient (in % of solvent B) was 0-5 min 20%, 5-20 min 70%, 20-30 min 20%. The flow rate was fixed at 1 mL min^{-1} and the injection volume was 50 µL. The acquisition was carried out in full-scan mode and concentrations determined against glyphosate and AMPA FMOC-derivatised standard curves ranging from 0 to 3 mM. Glyphosate and AMPA concentrations evolution were fitted to a three-parameter sigmoid model ($y= a/(1+\exp(-(x-x_0)/b)$ using Sigma plot Ver 11.0. Estimated parameters were *a* (maximal initial concentration), *k* (slope) and DT_{50} (time required for the concentration to decline (glyphosate) or increase (AMPA) to 50% of the maximum value). Fittings were performed separately for each sample replicate of each experimental treatment.

Apart from AMPA, other glyphosate metabolites (including sarcosine, glycine, and formaldehyde) were quantified at the beginning (Day 0), middle (Day 9), and late (Day 16)

phases of the glyphosate dissipation curve using commercial fluorescence assay kits (MAK073, MAK131, MAK261; Sigma-Aldrich) and following the manufacturer's instructions. At the end of the experiment (Day 18), glyphosate and AMPA were measured in the consortium biomass. Culture samples (30 mL) were dried and weighted before herbicide extraction using a custom method described by Carles et al. (2019).

Microbial biomass analyses

Chlorophyll-*a* concentration was determined from 5 mL of microbial culture at 4, 11, and 18 days. Chlorophyll-*a* was first extracted in 90 % acetone in the dark (24 h at 4 °C) and later sonicated (80 KHz, 4 min) to achieve complete extraction. Concentration of chlorophyll was determined spectrophotometrically after filtration (GF/F Whatman) of extracts and according to the calculations described by Jefferey & Humphrey (1975).

Bacterial densities were determined by flow cytometric counts (Borrel et al., 2012). One mL of microbial culture was placed in TE buffer (10 mM Tris, 1 mM EDTA) and fixed with paraformaldehyde (2% final concentration). Samples were treated with sodium pyrophosphate (10 mM final concentration) and incubated for 1 h at room temperature under orbital agitation (80 rpm). Then, bacterial suspensions were centrifuged at 800 *g* for 60 s and the supernatants diluted 10-fold and stained with SYBR Green I before counting bacterial cells with a BD FACSCalibur flow cytometer (15 mW at 488 nm, Becton Dickinson, U.S.A.).

Metabolism analyses

Metabolism of the microbial consortium was measured in glass incubation chambers of 15 mL. Net primary production (NPP, light chambers) and respiration (Resp, dark chambers) measurements were performed at 4, 11, and 18 days for all the experimental conditions tested. NPP and Resp were determined from the balance in oxygen concentrations after one hour incubation ($\Delta O_2 = O_2\, time_0 - O_2\, time_{1h}$) in sealed chambers. Incubations were always performed at 2:00 p.m. (maximum expected primary production rates) at constant air temperature (20 °C) and light (NPP = 1450-1500 Lux, Resp = 0 Lux) conditions and dissolved oxygen concentrations were measured using an oxygen meter (WTW, Germany). The oxygen balance (ΔO_2) in each chamber was converted into carbon units using the formula of the photosynthesis ($6\ CO_2 + 6\ H_2O \longrightarrow C_6H_{12}O_6 + 6\ O_2$) and further corrected by the amount of chlorophyll-a concentration in the chamber. Results were expressed in mg C µg chlorophyll-a^{-1} h^{-1}.

Dissolved organic carbon was measured in mid (Day 11) and late (Day 18) sampling dates in treatments were glyphosate was significantly transformed. One mL of these cultures was sampled and centrifuged at 13000 *g* during 5 min in order to pellet bacterial cells. The corresponding supernatants were diluted 10 times with ultrapure water and further analyzed on a TOC VCPN Analyser (Shimadzu, Japan).

Diversity analyses

Triplicate DNA extractions (10 mL microbial culture) per experimental treatment were performed at the end of the experiment (day 18) using the FastDNA™Spin Kit (MP Biomedicals, Irvine, CA) and following the manufacturer's instructions. The quantity and quality of the genomic DNA was determined spectrophotometrically (Nanodrop2000, Thermo Scientific™, Waltham, USA) and through 1% agarose gel electrophoresis. DNA samples were stored at -20°C until analysis. Sequencing (MiSeq bulk 2 x 250 bp, 10 M - 20 M paired reads on Illumina MiSeq) yielded a total of 1,563,836 reads (Eukaryotes) and 7,983,564 reads (Prokaryotes). Specific primers used for PCR were Euk_1391f (5'-GTACACACCGCCCGTC) / EukBr (5'-TGATCCTTCTGCAGGTTCACCTAC) for Eukaryotes and V4_515F_New (5'-GTGYCAGCMGCCGCGGTAA) / V4_806R_New (5'-GGACTACNVGGGTWTCTAAT) for Prokaryotes.

Statistical analyses

Two-way analysis of variance (ANOVA) tested differences among experimental treatments and time (as well as their interactions) for microbial variables (chlorophyll-a, NPP, Resp) measured at 4, 11, and 18 days. Post hoc multiple comparisons (Tukey's test) were run to test further differences among factor's levels for treatment and time. One way ANOVA was used to test differences among experimental treatments for density, diversity indices, and relative abundances of prokaryotes and eukaryotes, and for DT_{50} values of glyphosate and AMPA. No transformations were applied to our dataset since all descriptors fitted normal distribution. ANOVA analyses were performed with RStudio (Version 1.1.456).

Sample inference from amplicon data was carried out using DADA2 pipeline (Version 1.8). The DADA2 method consists in amplicon sequence variants (ASVs) inference instead of using OTU (Callahan et al., 2016). The corresponding sequence files were deposited to NCBI's Sequence Read Archive (PRJNA596462). Data analyses were performed using RStudio implemented with the Phyloseq package (version 1.24.0). Rarefaction curves were plotted using the ggplot2 package (version 3.0.0) from community analyses made with the

vegan package (version 2.5-2). After rarefaction, prokaryotic and eukaryotic datasets were each composed of samples containing the same number of reads (62871 reads for prokaryotes and 1257 reads for eukaryotes). Shannon index and Chao1 species richness, as well as hierarchical cluster analysis were performed on prokaryotic and eukaryotic assemblages using the Phyloseq package.

Results

Microbial biomass and metabolism of the consortium

After glyphosate-enrichment steps, the resulting microbial consortium adopted a greenish coloration suggesting that photoautotrophic organisms were present. Microbial development in the culture flasks during the 18-days experiment was determined from chlorphyll-*a* (chl-*a*) concentration and bacterial density measurements (Table 1). Chlorophyll-*a* concentration globally increased over the duration of the experiment ($P < 0.0001$), but this increase was dependent on the experimental treatment applied (Treatment x Time interaction, $P < 0.0001$). For instance, light treatments showed the highest increases on chlorophyll-*a* values over time (Light-Control and Light_Gly treatments, from 0.1 to 2.6 µg chl-*a* L^{-1} in average between days 4 and 18, respectively), though the addition of the antibiotic stopped chl-*a* increase (from 0.08 to 0.78 µg chl-*a* L^{-1} between days 4 and 18, respectively, in the Light_Gly_Antibiotic treatment) ($P < 0.05$, Table 1). Dark treatments had overall weak chl-*a* values comparing Light-Control and Light_Gly tratments, reaching values similar to those measured at the Light_Gly_Antibiotic treatment at day 18. Bacterial densities were only measured at day 18 and revealed consistently higher values in the Antibiotic treatments comparing to the rest of treatments (Tukey's test, $P < 0.05$; Table 1). Both in light and dark treatments, the supply of the antibiotic increased drastically the turbidity in culture flasks (Figure S2). Neither chl-*a* concentrations nor bacterial densities in the consortia were affected by the addition of the glyphosate.

According to microbial development in the culture flasks, the metabolism of the consortia also increased over time ($P < 0.0001$) depending on the experimental treatment (Treatment x Time interaction, $P < 0.0001$). Net Primary Production (NPP) was positive in light treatments (Production > Respiration) and negative in dark treatments (Production < Respiration), with the exception of the Light_Gly_Antibiotic treatment which experienced the lowest NPP ratio at Day18 (-14.54 +/- 2.75 mg C mg chl-a^{-1} h^{-1}) of the entire experiment

(Tukey's test, $P < 0.05$; Table 1). Although not statistically significant (Tukey's test, $P < 0.05$; Table 1), the herbicide glyphosate slightly decreased NPP rates of light treatments at days 11 (Light_control = 0.98 +/- 0.40 and Light_Gly = 0.51 +/- 0.34 mgC mg chl-a^{-1} h^{-1}) and 18 (Light_control = 1.31 +/- 0.76 and Light_Gly = 0.94 +/- 0.19 mgC mg chl-a^{-1} h^{-1}) comparing to controls. In contrast to NPP, respiration rates (Resp) tended to be higher in dark treatments at days 11 (Dark_control) and 18 (Dark_Gly) of the experiment, but again the Light_Gly_Antibtiotic treatment showed Resp rates close to those measured in the Dark_Gly treatment at Day 18 (Tukey's test, $P < 0.05$; Table 1). The herbicide did not affect respiration rates of dark and light treatments.

Glyphosate degradation by the consortium

Glyphosate concentrations measured at the beginning of the experiment (0.62 +/- 0.02 mM, average among treatments at day 0) were in the same range than the nominal concentration (0.6 mM). Glyphosate dissipation in the culture media followed a sigmoidal degradation kinetic in light and dark treatments, although the supply of antibiotics prevented its dissipation (Figure 1). In Dark_Gly and Light_Gly treatments, we observed a very slow dissipation during the first week followed by a drastic decrease (93-100% of the initial concentration) between days 7 to 11. Fittings to sigmoidal regression model revealed that DT_{50} values (time required for the glyphosate concentration to decline to 50% of the initial value) were similar between light and dark treatments (Tukey's test, $P < 0.05$; Table 2). Despite slope coefficients' fitting within the sigmoidal model regression was not statistically significant; these coefficients were slightly higher in dark than in light treatments (Table 2). In parallel to the degradation of glyphosate, the AMPA concentration in the media followed a drastic increase between days 7 to 11 to reach concentrations of 0.6 µM slightly lower than the glyphosate concentrations added at the beginning of the experiment; the transformation of glyphosate into AMPA being equimolar (Figure 1). AMPA concentrations were nearly zero in abiotic controls and antibiotic treatments. Analyses of further glyphosate's metabolites (sarcosine, glycine and formaldehyde) were performed at 0, 9, and 18 days of the experiment in Dark_Gly and Light_Gly treatments. Results revealed very low glycine and formaldehyde concentrations at day 0 ($\leq$ 5 µM) that were undetectable at days 9 and 18. Besides, sarcosine was never detected at any treatment and/or sampling time (data not shown).

Analysis of glyphosate and AMPA in the microbial biomass of cultures revealed very low accumulation at Day 18. Glyphosate concentration in the culture pellets was < 0.3 % of the amount of glyphosate supplied at the beginning of the experiment, while those of AMPA were

< 9% in terms of AMPA equivalents to glyphosate added. The non-negligible accumulation of AMPA in the microbial biomass of cultures could explain the difference between the initial glyphosate measured (0.62 +/- 0.02 mM) and the AMPA produced (0.6 mM) in the culture media at the end of experiment (Figure 1).

Microbial structure and composition of the consortium

The prokaryotic diversity of the consortium at day 18 was essentially dominated by representatives of the Proteobacteria phylum, but treatments consistently modified the structure of this prokaryotic assemblage (P <0.0001). The supply of glyphosate significantly enhanced the Shannon diversity of prokaryotes ASVs (3.20 +/- 0.24 and 2.93 +/- 0.15 in Dark_Gly and Light_Gly, respectively) when compared to control and antibiotic treatments, and this was irrespective of the light treatment (Tukey's test, $P < 0.05$; Table 3). In the same line, the cluster analysis (Figure S3) tended to separate the consortia receiving Glyphosate (including Dark_Gly and Light_ Gly) from those receiving the Gly_Antibio and Dark_controls (Bray-Curtis > 0.8, Figure S3). More precisely, the supply of glyphosate increased the relative abundance of Alphaproteobacteria in the consortium, especially the genus *Starkeya* (45.62 +/- 3.07 and 22.23 +/- 1.16 % relative abundance in Dark_Gly and Light_Gly treatments, respectively) when comparing to controls (1.03 +/- 0.38 and 0.08 +/- 0.04 % in Dark_Control and Light_Control treatments, respectively) (Tukey's test, $P < 0.05$; Figure 2). Further, *Phenylobacterium* sp. was the unique genus present in both Dark_Gly and Light_Gly treatments and absent in both Dark_Gly_Antibiotic and Light_Gly_Antibiotic. In contrast, the herbicide tended to decrease the relative abundance of Gammaproteobacteria (mainly *Pseudomonas* sp.) though these effects were not statistically significant.

The antibiotic decreased prokaryotes ASVs richness by 3.5 to 4.5 in comparison with treatments without antibiotic (Tukey's test, $P < 0.05$; Table 3). Despite Shannon indices based on ASVs were similar between controls and antibiotic treatments (Tukey's test, $P < 0.05$; Table 3), the supply of the antibiotic reduced classes diversity into an assemblage dominated by Gammaproteobacteria (99% sequences relative abundance corresponded to *Pseudomonas sp*., Figure 2) in both dark and light treatments. Finally, light availability separated communities in Light_Gly from Dark_Gly treatments (Bray-Curtis > 0.6, Figure S3) while this trend was less evident in communities treated with the antibiotic (Bray-Curtis < 0.1, Figure S3). Light significantly increased relative abundances of the Oxyphotobacteria class in Light_Control (31.5 +/- 14.6%) and Light_Gly (27.26 +/- 2.98%) treatments when comparing to dark and/or light_antibiotic treatments (Tukey's test, $P < 0.05$). After BLAST analysis,

sequences of Oxyphotobacteria corresponded to representatives of *Oscillatoriales* (data not shown).

The Shannon diversity indices of eukaryotes were much lower than those of prokaryotes in the consortium (Table 3). The eukaryotic assemblage was dominated by Chlorophyta, and more specifically by the *Trebouxiophyceae* class in both dark and light treatments (Figure 2). No significant impact of experimental treatments was observed in eukaryotes Shannon indices ($P = 0.064$). While the herbicide tended to enhance class richness of certain fungal classes (including Leotiomycetes, Chytridiomycota, Peronosporomycetes) in the Dark_Gly treatment, only Trebouxiophyceae sequences were detected in the Light_Gly treatment. The cluster analysis did not reveal clear trends structuring eukaryotic assemblages according to the imposed experimental treatments (Figure S3). Overall, the dissimilarity of eukaryotic communities among treatments (< 0.35) was much lower than that observed for prokaryotic communities (>0.8, Figure S3).

Discussion

In the present study, we investigated the influence of photoautotrophic DOM on the capacity of aquatic biofilm microorganisms in degrading the herbicide glyphosate. The dynamics of glyphosate dissipation in our experiment were similar to those observed in the study of Carles et al. (2019) using downstream biofilms of the Artière River from which our microbial consortium was isolated. However, the dissipation time (50%) in our consortium (DT_{50} = 9.46 +/- 0.25 days, average of dark and light treatments) was in the lower range of DT_{50} values obtained by Carles et al. (2019) (DT_{50} ranging 7.12 to 20.8 days), despite the fact that glyphosate concentrations used in our experiment (mg L^{-1}) were three orders of magnitude higher than those used by them (µg L^{-1}). This greater decay of glyphosate can reflect a greater specialization of glyphosate-degrading species in the consortium, since the latter was obtained from river biofilms after enrichment cultures with glyphosate (0.6, 10, 20 mM) as the main carbon source in the media.

Our study is among those few studies where the glyphosate has been tested as source of carbon for microbes (McAuliffe et al. 1990, Nourouzi et al. 2011, Zhao et al. 2015) rather than as source of phosphorous and/or nitrogen (see Sviridov et al. 2015). This specificity prompts a degradation pathway where the molecule of glyphosate is expected to be cleaved on the C–N bond by glyphosate oxidoreductase yielding stoichiometric quantities of AMPA and glyoxylate. Glyoxylate, as a convenient energy substrate, enters the glyoxylate bypass of the tricarboxylic acid cycle, while AMPA is exported into the extracellular space (Jacob et al.

1988) awaiting for further potential degradation (Rueppel et al. 1977). This was the main transformation pathway occurring in our experiment since glyphosate dissipation and AMPA formation in the media were at equal stoichiometric quantities at the end of experiment (Figure 1), though further AMPA decomposition and/or other metabolite production (including sarcosine, glycine, formaldehyde) was not observed. This transformation pathway was observed in both Light_Gly and Dark_Gly treatments but not when antibiotic was applied into the media.

The supply of chloramphenicol stopped the transformation of glyphosate indicating that chloramphenicol-sensitive bacteria were responsible of glyphosate transformation. The diversity analysis confirmed that prokaryotes ASVs richness drastically decreased when the antibiotic was added (from 61 to 13 and from 60 to 12 in the dark and light treatments, respectively). Specifically, the antibiotic reduced Alphaproteobacteria and Oxyphotobacteria classes' representatives, but not those of Gammaproteobacteria (Figure 2) among which the *Pseudomonas* sp. genus became dominant. Moreover, the highest bacterial densities in antibiotic treatments evidenced that *Pseudomonas* sp. grew better in the absence of competitors. The resistance to chloramphenicol has been already described by species of *Pseudomonas* (*i. e. Pseudomonas aeruginosa*) which can i) inactivate enzymatically the drug by means of acetylation, or ii) use specific exporters mediating resistance to chloramphenicol (Schwarz et al. 2004). The impossibility of *Pseudomonas* sp. in our experiment to transform the glyphosate in antibiotic treatments contrasted with the observations made for the same genus in soils. Gimsing *et al*. (2004) found a positive correlation between the population of *Pseudomonas* sp. in soils and the degradation rates of glyphosate (most probably through the AMPA degradation pathway) in these soils. The mismatch between our results and those from Gimsing *et al*. could be explained by the fact that chloramphenicol resistance and capacity of glyphosate degradation are characteristics not necessarily shared by the same *Pseudomonas* members.

Similar dynamics of glyphosate transformation were observed in Dark_Gly and Light_Gly treatments which confirm that light availability was not influencing glyphosate transformation. This result contradicts our hypothesis indicating that light availability would prompt photoautotrophs production and secretion of extracellular DOM which could, in turn, stimulate the biodegradation of glyphosate. Even if we observed greater chlorophyll-*a* concentration, net primary production, and slightly greater DOC concentrations in Light_Gly comparing to Dark_Gly treatments (38.68 ± 0.33 versus 36.6 ± 0.36 mg DOC L^{-1}), this was not sufficient to accelerate the biodegradation of glyphosate. In fact, assimilation ratios

measured in our experiment were relatively low (0.51 and 0.94 mg C mg chl^{-1} h^{-1} in the Light_Gly treatment at days 11 and 18, respectively) comparing to values found in the literature for plankton assemblages in lakes (*i. e.* 3-6 mg C mg chl^{-1} h^{-1} (Morabito et al. 2004) 1.75-2.5 mg C $mgchl^{-1}$ h^{-1} (Nõges and Kangro 2005)). This low production can also explain the low differences in DOC concentrations between light and dark treatments. To get rid of these limitations, further experiments should investigate how gradients of DOM production would influence glyphosate degradation by the microbial consortium.

Glyphosate strongly modified the structure and composition of prokaryotes in the consortium. The supply of glyphosate increased the relative abundance of *Starkeya* sp. (Alphaproteobacteria), and this increase was more marked in dark conditions than in light conditions. As facultative chemolithoautotroph, *Starkeya* sp. is capable to fix carbon from CO_2 and obtain energy from the oxidation of inorganic compounds already present in the media such as reduced sulphur (Kelly et al. 2000). Since chemolithoautotrophy is the dominant metabolism of *Starkeya* sp. their link with glyphosate transformation is difficult to establish in our experiment. Besides, the unique genus present in both Dark_Gly and Light_Gly treatments (capable to transform glyphosate into AMPA) and absent in both Dark_Gly_Antibiotic and Light_Gly_Antibiotic (not able to transform glyphosate) was *Phenylobacterium* sp.. *Phenylobacterium* is an Alphaproteobacteria belonging to Caulobacterales which metabolism is oligotroph and chemoorganotroph (Madigan et al. 2015) and could be linked to glyphosate transformation in order to obtain glyoxylate. In fact, *Phenylobacterium* species have been already described in the literature as capable to degrade herbicides (Lingens et al. 1985) and surfactants (Cortés-Lorenzo et al. 2013). To confirm if representatives of this genus were responsible of glyphosate transformation, further experiments based on isolation and enrichment culture techniques or using ^{13}C-labelled glyphosate approaches could be used.

In conclusion, the metabolism of glyphosate was not enhanced by auto-heterotrophic interactions in the aquatic microbial consortium. The relatively low DOM production levels and/or the potential interactions between degraders and non-degraders can explain the lack of differences in glyphosate degradation between light and dark conditions. Studies integrating different levels of biological complexity (from simplified microbial consortium to biofilm communities) are challenging in the field of aquatic microbial ecotoxicology in order to better understand the interplay among microorganisms during pesticides degradation.

Acknowledgments

This work was supported by the French National Research Agency in the frame of the project BIGLY (ANR-16-CE32-0001).

References

Bade DL, Carpenter SR, Cole JJ, Pace ML, Kritzberg E, Van de Bogert MC, Cory RM, McKnight DM (2007) Sources and fates of dissolved organic carbon in lakes as determined by whole lake carbon isotope additions. Biogeochemistry, 84:115–129

Borrel G, Colombet J, Robin A, Lehours AC, Prangishvili D, and Sime-Ngando T (2012) Unexpected and novel putative viruses in the sediments of a deep-dark permanently anoxic freshwater habitat. ISME J, 6: 2119–2127.

Callahan BJ, McMurdie PJ, Rosen MJ, Han AW, Johnson AJA, Holmes SP (2016). DADA2: High-resolution sample inference from Illumina amplicon data. Nature Methods, 13: 581–58.

Carles L, Gardon H, Farre M, Sanchis J, Artigas J (2019) Meta-analysis of glyphosate contamination in surface waters and dissipation by biofilms. Environ Int, 124: 284-293.

Carlson CA and Hansell DA. 2015. DOM Sources, Sinks, Reactivity, and Budgets. In: Biogeochemistry of Marine Dissolved Organic Matter. pp 65-126. doi:10.1016/b978-0-12-405940-5.00003-0

Cordero OX and Datta MS. 2016. Microbial interactions and community assembly at microscales. Curr Opin Microbiol, 31: 227-234.

Cortés-Lorenzo C, Sánchez-Peinado MM, Oliver-Rodríguez B, Vílchez JL, González-López JJ, Rodríguez-Díaz M (2013) Two novel strains within the family Caulobacteraceae capable of degradation of linear alkylbenzene sulfonates as pure cultures. Int Biodet Biodeg, 85: 62–65.

Espeland EM, Francoeur SN, Wetzel RG (2001) Influence of Algal Photosynthesis on Biofilm Bacterial Production and Associated Glucosidase and Xylosidase Activities. Microb Ecol, 42: 524-530.

Gimsing AL, Borggaard OK, Jacobsen OS, Aamand J, Sorensen J (2004) Chemical and microbiological soil characteristics controlling glyphosate mineralization in Danish surface soils. Appl Soil Ecol, 27: 233–242.

Horemans B, Vandermaesen J, Vanhaecke L, Smolders E, Springael D (2013) Variovorax sp.-mediated biodegradation of the phenyl urea herbicide linuron at micropollutant

493 concentrations and effects of natural dissolved organic matter as supplementary carbon
494 source. Appl Microbiol Biotech, 97: 9837-9846.
495 Jacob GS, Garbow JR, Hallas LE, Kimack NM, Kishore GM (1988) Metabolism of
496 glyphosate in Pseudomonas sp. strain LBr. Appl Environ Microbiol, 54: 2953–2958.
497 Jefferey SW and Humphrey UG (1975) New spectrophotometric equations for determining
498 chlorophylls a, b and c in higher plants, algae and natural phytoplankton.
499 BiochemPhysiol Pfl, 167: 191–194.
500 Kelly DP, McDonald IR, Wood AP (2000) Proposal for the reclassification of Thiobacillus
501 novellus as Starkeya novella gen. nov., comb. nov., in the a-subclass of the
502 Proteobacteria. Int J Syst Evol Microbiol, 50: 1797–1802
503 Kovárová-kovar K, Egli T (1998) Growth kinetics of suspended microbial cells: from single-
504 substrate-controlled growth to mixed substrate kinetics. Microbiol Mol Biol Rev,
505 62:646–666
506 Krüger M, Schledorn P, Schrödl W, Hoppe HW, Lutz W and Shehata AA (2014) Detection of
507 Glyphosate Residues in Animals and Humans. J Environ Anal Toxicol, 4:210 doi:
508 10.4172/2161-0525.1000210
509 Lingens F, Blecher R, Blecher H., Blobel F (1985). Phenylobacterium immobile gen. nov., sp.
510 nov., a gram-negative bacterium that degrades the herbicide chloridazon. Int J Syst
511 Bacteriol 35, 26–39.
512 Madigan MT, Martinko JM, Bender KS, Bickley DH, Stahl DA (2015) BROCK. Biology of
513 microorganisms 14th edition. Pearson Education, Madrid. 1136 p.
514 McAuliffe KS, Hallas LE, Kulpa CF (1990) Glyphosate degradation by Agrobacterium
515 radiobacter isolated from activated sludge. J Ind Microbiol, 6: 219–221.
516 Mee MT, Collins JJ, Church GM, Wang HH (2014) Syntrophic exchange in synthetic
517 microbial communities. PNAS, 111: 2149-2156
518 Morabito G, Hamza W, Ruggiu D (2004) Carbon assimilation and phytoplankton growth rates
519 across the trophic spectrum: an application of the chlorophyll labelling technique. J
520 Limnol, 63: 33-43.
521 Nourouzi MM, Chuah TG, Choong TSY, Lim CJ (2011) Glyphosate Utilization as the Source
522 of Carbon: Isolation and Identification of new Bacteria. E-Journal of Chemistry, 8:
523 1582-1587.
524 Nõges T and Kangro K (2005) Primary production of phytoplankton in a strongly stratified
525 temperate lake. Hydrobiologia, 547:105–122

526 Obojska A, Lejczak B, and Kubrak M (1999) Degradation of phosphonates by streptomycete
527 isolates. Appl Microbiol Biotechnol, 51: 872–876.
528 Pipke R, Amrhein N (1988) Isolation and Characterization of a Mutant of Arthrobacter sp. Strain
529 GLP-1 Which Utilizes the Herbicide Glyphosate as Its Sole Source of Phosphorus and
530 Nitrogen. Appl Environ Microbiol, 54: 2868-2870.
531 Rueppel ML, Brightwell BB, Schaefer J, Marvel JT (1977) Metabolism and degradation of
532 glyphosate in soil and water. J Agric Food Chem, 25:517–28.
533 Schwarz S, Kehrenberg C, Doublet B, Cloeckaert (2004) Molecular basis of bacterial
534 resistance to chloramphenicol and florfenicol. FEMS Microbiol Rev, 28: 519-542.
535 Shinabarger DL, Braymer HD (1986) Glyphosate catabolism by Pseudomonas sp. strain
536 PG2982. J Bacteriol, 168; 702–707.
537 Smith KEC, Thullner M, Wick LY, Harms H (2009) Sorption to humic acids enhances
538 polycyclic aromatic hydrocarbon biodegradation. Environ Sci Technol, 43:7205–7211.
539 Søndergaard M, Riemann B, Jorgensen NOG (1985) Extracellular organic carbon (EOC)
540 released by phytoplankton and bacterial production. Oikos 45: 323-332
541 Sviridov AV, Shushkova TV, Ermakova IT, Ivanova EV, Epiktetov DO, Leontievsky AA
542 (2015) Microbial degradation of glyphosate herbicides (Review). Appl Biochem
543 Microbiol, 51: 188-195.
544 Wang S, Liu B, Yuan D, Ma J (2016) A simple method for the determination of glyphosate
545 and aminomethylphosphonic acid in seawater matrix with high performance liquid
546 chromatography and fluorescence detection. Talanta, 161: 700–706.
547 Zhan H, Feng Y, Fan X, Chen S. (2018) Recent advances in glyphosate biodegradation. Appl
548 Microbiol Biotech, 102: 5033-5043.
549 Zhao H, Tao K, Zhu J, Liu S, Gao H, Zhou X (2015) Bioremediation potential of glyphosate-
550 degrading Pseudomonas spp. strains isolated from contaminated soil. J Gen Appl
551 Microbiol, 61: 165–170.
552
553
554
555

Table 1. Net Primary Production (NPP) and Respiration (Resp) rates corrected by chlorophyll-*a* (chl-*a*) concentration in the six experimental conditions tested at days 4, 11, and 18. Values of chl-*a* concentration are also supplied for the three sampling dates while bacterial density values are only available for day 18 (n.a. = not analysed). Values are means ± SE in parentheses (n=3). Statistical differences among treatments are marked by letters (a > b > c > d > e; Tukey's test, $P < 0.05$).

		NPP (mg C mg chl-*a*$^{-1}$ h^{-1})	**Resp** (mg C mg chl-*a*$^{-1}$ h^{-1})	**Chl-*a*** (µg chl-*a* L^{-1})	**Bacteria** (cells L^{-1})
Day4	Dark_Control	-0.04 (0.07) ^{a,b,c}	0.17 (0.06) ^{c}	0.18 (0.07) ^{d,e}	n.a.
	Dark_Gly_Antibiotic	-0.32 (0.17) ^{a,b,c}	0.20 (0.10) ^{c}	0.19 (0.02) ^{d,e}	n.a.
	Dark_Gly	-0.16 (0.03) ^{a,b,c}	0.14 (0.04) ^{c}	0.09 (0.01) ^{e}	n.a.
	Light_Control	0.13 (0.03) ^{a,b,c}	0.17 (0.02) ^{c}	0.16 (0.04) ^{d,e}	n.a.
	Light_Gly_Antibiotic	-0.56 (0.31) ^{a,b,c}	0.36 (0.11) ^{c}	0.08 (0.01) ^{e}	n.a.
	Light_Gly	0.24 (0.09) ^{a,b,c}	0.18 (0.07) ^{c}	0.09 (0.04) ^{e}	n.a.
Day 11	Dark_Control	-0.71 (0.27) ^{a,b,c}	7.52 (0.86) ^{a}	0.54 (0.04) ^{b,c,d,e}	n.a.
	Dark_Gly_Antibiotic	-0.11 (0.78) ^{a,b,c}	2.27 (0.40) ^{b,c,d}	1.13 (0.10) ^{b,c}	n.a.
	Dark_Gly	-1.64 (0.16) ^{b,c}	4.23 (0.65) ^{a,b,c}	0.50 (0.04) ^{c,d,e}	n.a.
	Light_Control	0.98 (0.40) ^{a,b}	3.28 (0.13) ^{b,c,d}	1.20 (0.04) ^{b}	n.a.
	Light_Gly_Antibiotic	-0.05 (0.29) ^{a,b,c}	3.18 (0.88) ^{a,b,c,d}	1.20 (0.34) ^{b}	n.a.
	Light_Gly	0.51 (0.34) ^{a,b,c}	3.94 (0.29) ^{a,b,c,d}	0.97 (0.04) ^{b,c}	n.a.
Day 18	Dark_Control	-3.93 (0.89) ^{c}	3.89 (0.86) ^{a,b,c,d}	0.66 (0.04) ^{b,c,d,e}	1.22×10^{9} (6.09×10^{7}) ^{b}
	Dark_Gly_Antibiotic	-2.05 (1.92) ^{b,c}	1.41 (0.81) ^{c,d}	0.70 (0.07) ^{b,c,d,e}	2.71×10^{11} (4.42×10^{10}) ^{a}
	Dark_Gly	-3.53 (0.83) ^{b,c}	5.96 (1.77) ^{a,b}	0.70 (0.13) ^{b,c,d,e}	4.19×10^{9} (5.29×10^{8}) ^{b}
	Light_Control	1.31 (0.76) ^{a}	2.78 (1.40) ^{b,c,d}	2.64 (0.16) ^{a}	2.45×10^{10} (1.91×10^{10}) ^{b}
	Light_Gly_Antibiotic	-14.54 (2.75) ^{d}	6.09 (0.84) ^{a,b}	0.78 (0.14) ^{b,c,d}	9.87×10^{10} (2.95×10^{10}) ^{b}
	Light_Gly	0.94 (0.19) ^{a,b}	2.34 (0.25) ^{b,c,d}	2.56 (0.27) ^{a}	4.92×10^{9} (6.62×10^{8}) ^{b}

Table 2. DT_{50} (time required for the concentration to decline (glyphosate) or increase (AMPA) to 50% of the maximum value, DT_{50}) and k (slope) parameters estimated from glyphosate dissipation and AMPA production curves (mean (SE)). Fittings of glyphosate and AMPA data to three-parameter sigmoid model are represented by R^2 and P-values. Specific P-values for curve coefficients (DT_{50} and k) were only significant for DT_{50} ($P < 0.05$). Accordingly, statistical differences among treatments were only calculated for DT_{50} (letters : a > b; Tukey's test, $P < 0.05$).

		DT_{50} (days)	k	R^2	P-value
Glyphosate	Dark_Gly	9.26 (0.02) [a]	-1.04 (0.13)	1	< 0.0001
	Light_Gly	9.41 (0.24) [a]	-0.62 (0.01)	1	< 0.0001
AMPA	Dark_Gly	9.28 (0.02) [a]	0.89 (0.07)	1	< 0.0001
	Light_Gly	9.64 (0.53) [a]	0.52 (0.07)	1	< 0.0001

Table 3. Diversity indices based on ASVs from the 16 S and 18S rRNA of the consortium subjected to the six different treatments at the end of the experiment (day 18). The ASVs richness (*Rich*) and diversity (Shannon index, *H*) is represented as mean values (n = 3) and standard error in parenthesis. Statistical differences among treatments are marked by letters (a > b > c > d > e; Tukey's test, $P < 0.05$).

Microbial community	Treatment	*Rich*	*H*
16 S rRNA	Dark_Control	52 (7) [a]	1.73 (0.18) [b]
	Dark_Gly_Antibiotic	13 (2) [c]	1.77 (0.15) [b]
	Dark_Gly	61 (2) [a]	3.20 (0.24) [a]
	Light_Control	44 (14) [a,b]	2.11 (0.12) [b]
	Light_Gly_Antibiotic	12 (1) [c]	1.65 (0.13) [b]
	Light_Gly	60 (1) [a]	2.93 (0.15) [a]
18 S rRNA	Dark_Control	3 (1) [b]	0.24 (0.14) [a]
	Dark_Gly_Antibiotic	3 (1) [b]	0.46 (0.24) [a]
	Dark_Gly	8 (2) [a]	0.62 (0.20) [a]
	Light_Control	3 (0) [b]	0.25 (0.12) [a]
	Light_Gly_Antibiotic	2 (0) [b]	0.22 (0.03) [a]
	Light_Gly	3 (0) [b]	0.11 (0.01) [a]

Figure 1. Glyphosate and AMPA concentrations evolution during the experiment. Concentrations (in µM) are expressed by means (n=3) and standard errors for treatments receiving glyphosate (Abiotic controls, Gly_Antibio, and Gly in light and dark conditions) at the different sampling times.

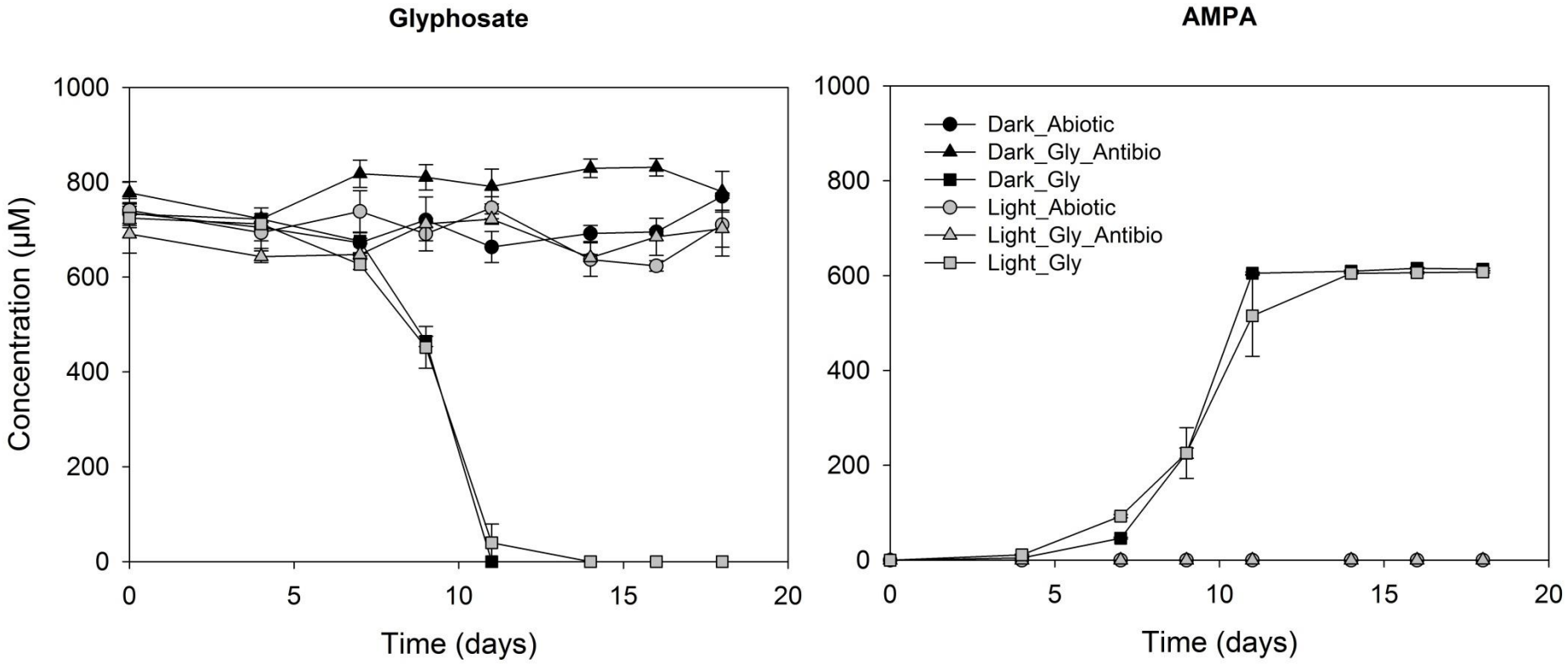

Figure 2. Relative abundances of prokaryotes and eukaryotes classes in the six experimental treatments at day 18. Values are means (n = 3) and standard errors. Statistical differences among treatments are marked by letters (a > b > c > d > e > f; Tukey's test, $P < 0.05$).